



**AIAA-2002-0366**

**ACOUSTIC SOURCE LOCALIZATION USING A 3-D  
MICROPHONE ARRAY IN A MACH 1.3 JET**

**James Hileman, Brian Thurow and Mo Samimy**

**The Ohio State University  
Department of Mechanical Engineering  
Columbus, OH 43210**

**40th Aerospace Sciences  
Meeting & Exhibit  
January 14 - 17, 2002/ Reno, NV**

## Acoustic Source Localization Using a 3-D Microphone Array in a Mach 1.3 Jet

J. Hileman<sup>1</sup>, B. Thurow<sup>2</sup>, and M. Samimy<sup>3</sup>  
 Department of Mechanical Engineering  
 The Ohio State University, Columbus, Ohio 43210

A 3-D microphone array was developed and used to locate the origins of individual sound waves that were created within a high-speed and high Reynolds number turbulent jet. In previous work by the authors, a linear array of microphones and simultaneous temporally resolved flow visualizations were used to determine the origin of individual sound waves and their generation mechanisms within the jet. The linear array algorithm assumed the noise sources were distributed along the jet axis, and the array was not equipped to deal with an off axis distribution of noise sources. Further, the registration of sound radiation from similar events within the mixing layer was observed to depend on whether the events occurred on the array side of the jet or the opposite side. Based on these error sources and observations, a new array was developed that can locate the individual sources of sound waves within three dimensions. This work presents the development of this array, its validation using a Hartmann tube fluidic actuator (HTFA), and its use to locate noise sources within a Mach 1.3 jet. The 3-D array and its accompanying noise source location algorithm appear to be quite robust and accurate as they accurately predicted the location of noise sources from an HTFA and the expected radial distribution of noise sources of a high-speed jet. The array will be used with simultaneous temporally resolved flow visualizations to further explore jet noise sources.

### Introduction

This paper presents progress of an ongoing work that is being conducted on an ideally expanded Mach 1.3 axisymmetric jet. The purpose of the work is to relate the development and interaction of large structures within the jet's mixing layer to radiated far field noise. This paper presents the development and use of a three-dimensional microphone array that will be used to perform laser based flow diagnostics with simultaneous far field acoustic measurements for noise source localization. Some of the pertinent results from previous papers<sup>1-3</sup> will be reviewed in this introduction as well as other papers that directly relate to the development of the array.

The far field noise for the Mach 1.3 jet used in this study is most intense at an angle of 30° with respect to the downstream jet axis at a frequency of about 3 kHz ( $St_D = 0.2$ ).<sup>1</sup> Since the most intense noise was being recorded at an angle of 30°, an inline array of four microphones was placed at this orientation in the far field to determine where this sound was being created.<sup>2</sup> The origin of individual sound waves were determined using the phase lag between individual microphones recording the sound wave of interest. The origin for every sound wave that had a magnitude in excess of 1.5 times the standard deviation of the overall

measured sound was resolved. The majority (70%) of the sound was being created between 5 and 10D.<sup>2</sup> This is in agreement with the results of other researchers using other techniques.<sup>4-7</sup> By utilizing various microphone arrays, several research groups have found that the high-frequency noise from high subsonic jets is generated near the nozzle exit, while lower-frequency noise originates farther downstream.<sup>8-10</sup>

Individual noise source locations were compared in to simultaneously taken temporally resolved flow images.<sup>1-3</sup> The visualizations consisted of seventeen planar images of the flow with a time separation of 10  $\mu$ s. Based on these results, two mechanisms of sound generation were identified: cross mixing layer interaction and the roll-up of large structures.<sup>2,3</sup> A third, much less frequently occurring mechanism of noise generation, large structure tearing, was also observed in prior work.<sup>1</sup>

There are two issues with the inline microphone array used in references 1-3. One of the underlying assumptions was that the noise sources were distributed along the jet centerline. Another was that refraction of acoustic waves within the jet could be neglected. Further, the acoustic radiation to the far field was assumed to be axisymmetric. As discussed in reference 1, the assumption of a centerline distribution

<sup>1</sup> Graduate student, OSGC Fellow, member AIAA

<sup>2</sup> Graduate student, NDSEG Fellow, member AIAA

<sup>3</sup> Professor, Associate Fellow AIAA

Copyright © 2002 by James I. Hileman. Published by the American Institute of Aeronautics and Astronautics, Inc. with permission.

of noise sources added 0.9 D error to the overall error in the streamwise noise source location (this assumed a possible error of  $\pm 0.5 D$  in radial distance).

One observation from reference 2 was that structure roll-up within the top half of the mixing layer (the side where the array was located) registered intense noise emission while an equivalent structure roll-up within the bottom half of the mixing layer did not. This observation raises the question of whether this is due to refraction of sound wave within the jet or due to asymmetric radiation. A preliminary exploration of this issue was carried out in reference 2. In that work, two separate inline arrays (each array consisted of two microphones) were used to analyze the noise signals in the time domain. One microphone pair was placed above the jet at the  $30^\circ$  location, while the other pair was located below the jet directly under the top pair. Sometimes, sound waves reached the top and bottom microphones at the same time as would be expected if the source were on the jet centerline and it had an axisymmetric radiation pattern. In some other instances, there was a time separation between a sound wave reaching the top and bottom microphones and also attenuation of one with respect to the other; this would result if the noise source was located a radial distance from the jet centerline. Furthermore, there were also cases in which either the top or bottom microphones registered an intense sound. This could point to severe refraction, non-axisymmetric radiation, or a combination thereof. Reference 11 explores and discusses acoustic refraction in a jet using numerical simulations.

Based on the inherent problems using an inline array to determine instantaneous noise source locations within a jet and the observed azimuthal variations in the sound waves, a microphone array needed to be developed that could identify the location of noise sources in three-dimensions. This paper discusses the development, evaluation, and application of such an array. The remainder of this paper can be divided into three parts: 1) the development of a 3-D microphone array with inline and azimuthally distributed elements, 2) the validation of the array using a Hartmann tube, and 3) a presentation and discussion of the results using this array in a Mach 1.3 jet.

### The 3-D array

#### *Design of the Array*

To measure noise source origins in three dimensions, one has to have a distribution of microphones in space. With an inline array, only a linear distribution of noise sources can be resolved. An azimuthal distribution of microphones would be able to determine the noise source locations azimuthally, but

not axially. If this azimuthal array is used in conjunction with an inline array that is normal to the plane of the azimuthal array, then the three components of the noise source location can be determined. Therefore, both an azimuthal and a linear distribution of microphones will be used to resolve the location of the noise sources in three dimensions.

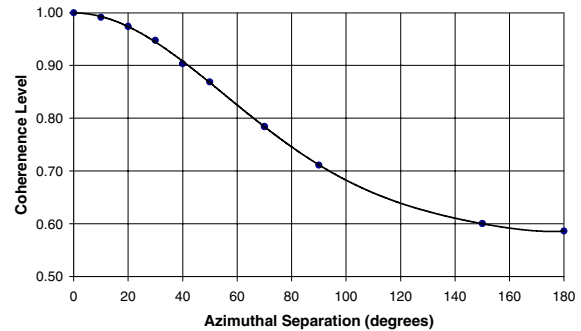


Figure 1: Coherence levels at  $30^\circ$  for various azimuthal microphone separations (frequency band of 2 to 4 kHz).

The 3-D array will eventually be used with simultaneous flow visualizations in the streamwise plane. Thus, the focus will be on the top and bottom regions of the jet's mixing layer, and the array should have maximum sensitivity to these regions. The azimuthal distribution of microphones needs to encompass as large an area as possible without significant loss of sound wave coherence. To determine what this separation should be, the coherence level between the radiated sound that was recorded at different azimuthal microphone separations was measured. The microphones were at a  $30^\circ$  downstream location and the coherence level was averaged over frequencies between 2 and 4 kHz to yield the curve presented in Figure 1. The choice of this frequency range came from our earlier results that show the broadband peak frequency at  $30^\circ$  is between 2 and 4 kHz.<sup>1</sup> Since the coherence level is quite high for the  $60^\circ$  separation (over 0.8), and there were eight  $\frac{1}{4}$  inch microphones available, six equally spaced azimuthal locations, three on top and three at the bottom were chosen for this work. At the top ( $0^\circ$ ) and bottom ( $180^\circ$ ) microphone locations, a second microphone was placed 7.5D behind the front microphone. Figure 2 shows a schematic of the microphone locations with respect to the jet exit. The rest of this paper uses the conventions of this figure. Such a large spacing between inline microphones has been used in previous arrays without any problem.<sup>3</sup> The array was also designed to allow a wide variety of microphone separations (in both the downstream and azimuthal directions).

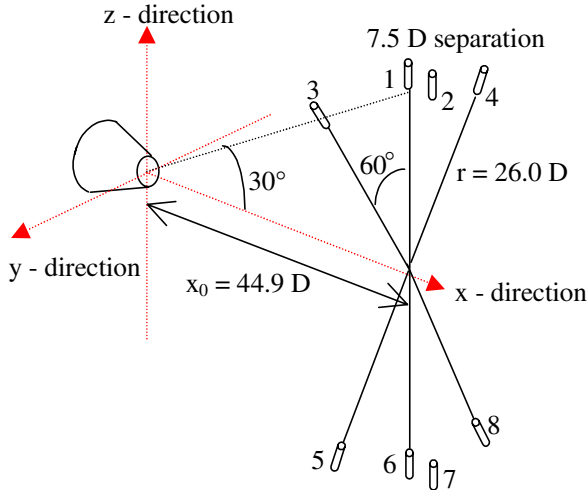


Figure 2: Schematic of the microphone locations in the 3-D array.

The backbone of the 3-D array is an inch thick ring of aluminum that is shown in the drawing of Figure 3. It has an inner diameter of 60 inches and an outer diameter of 66 inches. The inner diameter was held to a tolerance of 10 thousandths of an inch. Dual sets of holes (radial separation of 2 inches) were drilled around the periphery of the ring at 10° increments as well as the multiples of 45°. The array is mounted to the floor and ceiling via the top and bottom sets of holes within the aluminum ring. Guide wires connected to the walls of the anechoic chamber hold the sides of the array fixed. The hole sets were designed to facilitate custom-built, precision microphone mounts.

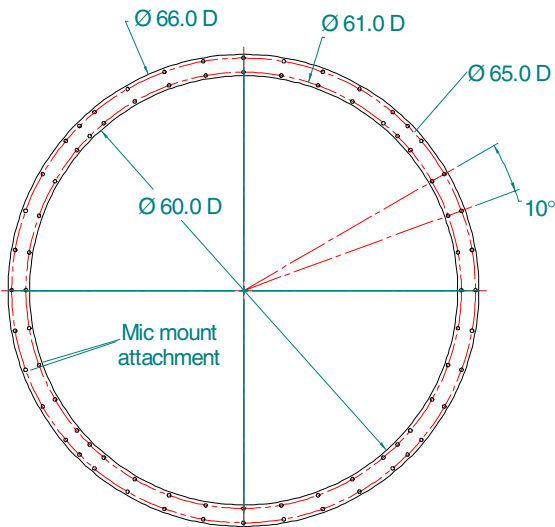


Figure 3: Drawing of the ring of the 3-D array.

The azimuthal mounts hold a single microphone at a fixed distance from the inner radius of the ring. Figure 4 shows a drawing for the microphone

mount. The distance from the inside of the ring to the diaphragm of the microphone can be precisely measured and fixed by a set screw. Therefore, the distance from the microphone to the jet centerline is controlled by how accurately the ring can be centered on the jet centerline. Furthermore, since these mounts have a fixed extension post, the distance from the ring face to the microphone center is set, and the downstream distance from the exit of the nozzle to the microphones is determined by the placement of the ring.

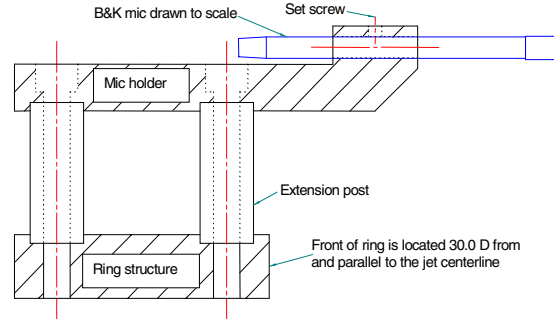


Figure 4: Drawing of a microphone mount for the azimuthal positions.



Figure 5: Picture of the arc array in the anechoic chamber. It has been wrapped in acoustic foam.

The inline microphones are housed in aluminum blocks that are attached to the mounting brackets at the top and bottom of the ring. The height of the pedestals used in the azimuthal mounts was selected to match the distance from the front microphone of the inline array to the front of the ring

backbone. Hence, all six azimuthally distributed microphones are at the same downstream location. Figure 5 shows a picture of the arc array within the anechoic chamber.

#### Noise Location Algorithm

The principles behind the 3-D array are the same as those used in our earlier work.<sup>1</sup> In that work, the delay between when a sound wave passed two microphones (phase lag) was used to determine noise source location within the jet. With the delay and the knowledge of the geometry of the experiment, the flight path of the wave along the direction of the microphones was determined.<sup>1-3</sup> The same principle is now being extended to microphones in three dimensional space to determine the acoustic wave flight path in space.

The first step in the noise location algorithm is to identify sound waves that are of interest. The sound data is normalized by its standard deviation to facilitate easier examination. Then all sound pressure peaks that have a magnitude above 1.5 are identified and the time of the relative maxima is recorded. Since this peak time is going to be in the center of a correlation window and then another microphone's signal is going to be scanned for correlation, some data points at the front and end of each data set are not examined for maxima. Therefore, more data is taken than is actually analyzed for noise source locations.

The time delay is determined by finding the maximum value of the correlation coefficient,  $\rho_{ab}$ , between two microphone signals,  $a$  and  $b$ . The correlation coefficient is given by:

$$\rho_{ab}(\tau) = \frac{\langle a(t)b(t+\tau) \rangle - \mu_a \mu_b}{\sigma_a \sigma_b} \quad (3)$$

where  $\langle \rangle$  is the time average,  $\tau$  is a time delay,  $\sigma$  is the standard deviation, and  $\mu$  is the mean. The correlation coefficient is only computed over a range of values of  $\tau$  that are realistic, i.e. those delays that would be expected if the sound had originated within an area surrounding the jet. The signal length chosen for correlation was 350  $\mu$ s. This length was chosen since it would contain a single sound pressure peak.

An algorithm had to be established that could take the time delays and then determine where the noise source was located. After some exploration, it was decided to use the location vectors of the microphones in conjunction with an iterative routine to determine the apparent noise source location,  $\vec{S} = [x_s, y_s, z_s]$ . The jet exit center is set as the origin.

If the location of a noise source were known, then the time delay between a sound wave reaching two

microphones 'i' and 'j',  $dt_{ij}$ , could be determined by the following vector equation:

$$dt_{ij} = t_i - t_j = \frac{|\vec{M}_i - \vec{S}| - |\vec{M}_j - \vec{S}|}{c} \quad (4)$$

where  $t_i$  is the time microphone 'i' recorded the peak of the sound wave,  $\vec{M}_i$  is the vector location of microphone 'i,'  $\vec{M}_j$  is the vector location of microphone 'j,'  $c$  is the speed of sound within the medium surrounding the sound source, and  $|\bullet|$  is the norm of a vector. Since  $dt_{ij}$  is known, but  $\vec{S}$  is not, the appropriate approach is to find what value of  $\vec{S}$  causes  $Q_{dummy}$  to be equal to zero in the following equation:

$$Q_{dummy} = \frac{|\vec{M}_i - \vec{S}| - |\vec{M}_j - \vec{S}|}{c} - dt_{ij} \quad (5)$$

An initial value for  $\vec{S}$  is assumed for the noise source with one of the components varied to find what value will render  $Q_{dummy}$  equal to zero. If the value of the component returned from this procedure was out of the range of expected values, the previous value was used instead. Now that the procedure of finding the noise source location from a time separation has been determined, the next question is, "which microphone pairs (i-j) should be used to determine the source location?"

The azimuthally distributed microphones have to be used to determine the y- and z-components of the noise source (see Figure 2 for the coordinate system used). The iterative routine starts with the determination of the z-component, and later that value is used to compute the y-component. The best choice of microphone pairs for the z-component would be those microphones that straddle the  $y = 0$  plane. Thus, microphone pairs 4 & 8 and 3 & 5 are used. Equation 5 is first used with  $i$  equal to 4 and  $j$  equal to 8 to determine a value for the z-component. This is then repeated with  $i$  equal to 3 and  $j$  equal to 5 to determine another value for the z-component. In both cases, the initial guess for  $\vec{S}$  was  $[0, 0, 0]$ . The two values for the z-component are then averaged to get the first iteration value for  $z_s$ .

The determination of the x and y components of  $\vec{S}$  must rely on a pre-existing knowledge of the z-location of the noise source. This is due to the previously described refraction effect. The most accurate measure of the flight path will be on the side

of the jet mixing layer that contains the noise source. The z-component result from the previous paragraph could be used for this purpose, but there is a more accurate method. Instead, the time delay between opposite inline microphones can be used. If the time delay between the front, inline microphones,  $dt_{16}$ , is negative, then the sound wave of interest reached the top microphone before the bottom and the sound originated above the jet centerline. As a check of  $dt_{16}$ , the time delay between the rear, inline microphones,  $dt_{27}$ , is also determined. If both  $dt_{16}$  and  $dt_{27}$  are negative, then the source of the sound was above the jet centerline. The opposite case also holds. Refraction should be beneficial in this regard since any wave that is refracted will take longer to reach its destination than would a wave that was not refracted. Hence, the delay between a refracted wave reaching one microphone and the unrefracted wave leaving the opposite side toward the opposite microphone would be even larger than if neither wave had been refracted. If  $dt_{16}$  and  $dt_{27}$  do not have the same sign, then the previously computed value of  $z_s$  is used to determine which side of the jet contained the noise source.

The only way to determine  $x_s$  is to use the time delay between the inline microphones. Let's assume the analysis of the previous paragraph predicted the noise source was located above the jet centerline. In this case, the top set of inline microphones would be used to determine the x-component of the noise source location. Equation 5 is then used with an initial guess of  $[0, 0, z_s]$  for  $\vec{S}$ , and  $i$  and  $j$  are set, respectively, to 2 and 1. If the noise source was below the jet centerline,  $i$  and  $j$  would be set, respectively, to 7 and 6. In either case, the result is the value for the first iteration of  $x_s$ .

The y-component of the noise source is determined based on the microphone pairs that straddle the  $z = 0$  plane. Unlike the z-component equations, there are three microphones on both the top and bottom of the ring that meet this requirement. Along the top of the ring, these pairs are 4 & 1 and 3 & 1; on the bottom, they are 8 & 6 and 5 & 6. Which pair is used depends on whether the noise source is above or below the jet centerline (this determination is the same as that used in the above x-component computations). If the noise source were determined to be above the jet centerline, equation 5 would be used with an initial guess for  $\vec{S}$  of  $[x_s, 0, z_s]$  and the values of  $i$  and  $j$  would be 4 and 1 to get one value for the y-component, and then this is repeated with  $i$  and  $j$  equal to 3 and 1. These two y-components are then averaged to get  $y_s$ . If the noise source were below the jet centerline, the microphone values for  $i$  and  $j$  would be 8 and 6 for the one pair and 5 and 6 for the other pair. With the value for  $y_s$ , the first iteration is complete.

After the first iteration is complete, a second iteration is automatically started. The coordinates for  $\vec{S}$  from the first iteration are used as the initial guess for the second iteration. Additional iterations are performed with the value of  $\vec{S}$  from the previous iteration as the new initial guess until the difference between subsequent values for all three coordinates are less than 0.1 %. If the routine reaches fifty iterations without convergence, then all three components of  $\vec{S}$  are set to 99.9 and the results are discarded.

#### *Error Analysis*

A preliminary error analysis was conducted. The error sources were broken up in the following manner:

- 1) Accuracy in the microphone placement relative to the ring structure, the ambient conditions within the anechoic chamber, and the measurement of the time delays.
- 2) Accuracy in the placement of the ring structure with respect to the jet centerline and nozzle exit.
- 3) Other errors that can only be speculated upon at this point.

The sources within the first two listed items are discussed in detail within Appendix A. Each of the uncertainties was varied to yield a worst case scenario that gave a maximum deviation for a set of time delays. Based on that preliminary analysis, the uncertainty in the streamwise direction (x-component) for this array would be about 1 D while the uncertainties in the y and z-components would be negligible.

These values are a vast improvement over the estimated uncertainties for the linear arrays used in references 1-3. The array of reference 1 had an estimated worst-case uncertainty in the streamwise location of +/- 2.5 D. Although not published elsewhere, the linear array of references 2 and 3 had an estimated uncertainty of +/- 2.0 D in the noise source location. A large portion of the uncertainty for both of these inline arrays came from the centerline assumption, which has been eliminated with the present configuration.

As mentioned in item 3, there are also other sources of uncertainty that are not known. The biggest and the only one mentioned in this work, is the effect of refraction on the flight path of a sound wave as it travels through the mixing layer of the jet. This error source is minimized by first determining which side of the jet contained the noise source, and then using microphones that are on that side of the jet to compute the x and y-components of the noise source. The dominant wavelengths of the overall sound field are

between 3 and 7 D (wavelengths for frequencies between 2 and 4 kHz), which are much larger than the flow scales of the jet. Since the wavelengths of interest are much larger than the flow scales of interest, and the locations for the noise sources are on the same side of the jet as the microphones used to locate their source, refraction should not have a large effect on the predicted noise source locations.

#### *Microphone Equipment*

The microphones used in the experiments are either Bruel & Kjaer 4135 or 4939 ¼ inch condenser microphones. The microphones are connected to Bruel & Kjaer 2633 or 2670 preamplifiers. Four of the microphones are connected to two 5935 amplifiers and then frequency filters. The other four microphones are connected to a Bruel & Kjaer Nexus conditioning amplifier. Two National Instruments PC-6110E data acquisition boards were used within a Pentium II computer to collect the data. The two boards were operated in simultaneous acquisition mode via an internal RTSI connection. The data was acquired with Labview.

#### *Anechoic Chamber*

The optically accessed anechoic chamber of the Gas Dynamics and Turbulence Laboratory was used to conduct the array experiments. The chamber was tested for compliance to ANSI Standard S12.3535, and the results from the tests were within the required tolerance over most of the distances along the microphone paths.<sup>12</sup> The inner dimensions of the chamber measure, from wedge tip to wedge tip, 3.12 meters in width and length, and 2.69 meters in height. Additional details of the anechoic chamber and jet flow facility can be found in references 1 and 12.

#### **Hartmann Tube Validation**

A Hartmann tube based fluidic actuator (HTFA), designed within our laboratory, was used to test ability of the 3-D array to locate sound sources.<sup>13</sup> A Hartmann tube consists of an underexpanded jet and a closed-ended tube where the open end of the tube is placed within a compression region of the underexpanded jet.<sup>14</sup> An HTFA is created by placing a cylindrical shield between the nozzle and the tube that covers a large portion of the open area.<sup>15</sup> The HTFA used in this validation created a pure acoustic tone with a frequency of 2124 Hz along with three harmonics. The opening of the HTFA was a square with sides equal to 8 mm. Further details of the HTFA experiment are included in Appendix B. The results that are pertinent to the validation of the array are discussed in the following paragraph.

The noise producing area of the HTFA had narrow y and z distributions, but they both had a slight offset from the opening of the HTFA. The distribution in the x-direction was as expected with 98 % of the noise created between the exit of the tube and a location that was 32 mm downstream of the opening. The offset in the y and z directions could be caused by a slight difference in the center of the microphone ring and the actual jet centerline. To check this, the locations of the microphones were offset in the noise source location codes by - 0.17 inch in the y-direction and by - 0.28 inch in the z-direction. This effectively shifted the location of the ring center to match the predicted center of the HTFA opening, which was aligned with the jet centerline. The noise source locations were then recomputed with these new microphone locations. The correction resulted in y and z distributions that were offset from the origin by 0.02 and 0.03 inch, respectively, and the distribution in the x-direction was not significantly altered by the change in the microphone locations. Thus, it appears that the location of the center of the ring that supports the microphones within the 3-D array was slightly offset from the actual jet centerline. The results from the Mach 1.3 jet will further support this offset in the microphone locations.

#### **Jet Noise Source Localization**

##### *Jet Facility*

The air for the Mach 1.3 jet is supplied by two four stage compressors; it was filtered, dried, and stored in two cylindrical tanks with a total capacity of 42.5 m<sup>3</sup> at a pressure of 16.5 MPa (1600 ft<sup>3</sup> at 2500 psi). A stagnation chamber was used to condition the jet air before exhausting it through a 25.4 mm (1 inch) nozzle with a lip thickness of 2.5 mm (0.1 in) where the inner contour was determined by the method of characteristics for uniform flow at the exit. The actual Mach number of the nozzle was measured as 1.28. The Reynolds number for the jet was slightly above 10<sup>6</sup>.

##### *Microphone Checks using the Mach 1.3 Jet*

The purpose of designing this 3-D array is to determine noise source locations within a jet with simultaneous flow visualization. The work presented here is a step toward that goal. The results of this work will be used for an analysis of the average properties of the mixing noise from the Mach 1.3 jet and as a further test of the 3-D array's ability to determine noise source locations.

The average sound pressure level was computed for frequencies between 200 Hz and 30 kHz to search for additional unknown error sources within the array setup. Since the microphones were all at a fixed distance from the inner radius of the ring and six of the eight were at the same downstream location,

these six microphones were expected to record the same average sound pressure level. This data set consisted of 100 blocks of 4096 samples taken at a sample rate of 100 kHz with low pass filtering applied at 30 kHz. The average Sound Pressure Level (SPL) values are presented in Table 1. The inline microphones (microphones 1, 2, 6, and 7, all located at 0° and 180° azimuthally; see Fig. 2) had an average SPL of 95.1 dB with a spread of 0.25 dB. The azimuthally distributed microphones (3, 4, 5, and 8) had an average SPL value of 93.2 with a spread of 0.35 dB.

Microphone number (Fig. 2)	Average SPL between 200 Hz and 30 kHz (dB)
1	94.94
2	95.20
3	93.03
4	93.38
5	93.05
6	95.10
7	95.19
8	93.22

Table 1: Sound Pressure Level (SPL) values recorded by the eight microphones comprising the array.

The difference between the inline and azimuthal microphones sound pressure levels is a cause for concern. Since the microphone signals for microphones 1 & 4 were sent through the Nexxus signal conditioner and microphones 5 & 8 went through the older amplifiers and filters, the difference is not likely hardware related. The cause is likely related to the manner in which the microphones were mounted. The azimuthally distributed microphones had mounts like that shown in Figure 4. The ends of these microphones were an inch beyond the acoustic foam. The inline microphones were housed in the microphone blocks where only ¼ inch of the microphone was above the acoustic foam (the foam itself is over an inch thick to minimize acoustic reflections off of the block surface). This issue will receive further future examination.

### 3-D Noise Source Location within the Mach 1.3 Jet

A large data set was taken for noise source location analysis of the Mach 1.3 jet. The data set consisted of 200 blocks of 16384 samples taken at a sampling frequency of 1 MHz. The data was low pass frequency filtered at 100 kHz. Within the 2.5 seconds of data, there were 7774 sound waves with a magnitude larger than  $1.5 \sigma$  (the standard deviation of the sound pressure level), and the apparent origin for each of these sound waves was determined. Unless otherwise specified, all noise source locations discussed were

based on the  $1.5 \sigma$  threshold. The microphone locations used for the noise source location calculations were modified by the y and z offsets used for the HTFA validation.

The x component of the noise source location has been plotted in the form of a probability density distribution in Figure 6. It was created using a bin size of 1 D with bins ranging from -5 to 25 D. Each bin was centered on an integer, i.e., the bin at zero covers -0.5 to +0.5 D. There were only ten instances (out of 7774 noise source locations) where the array predicted a noise source upstream of the nozzle exit. This is expected as there should not be any significant sound generated upstream of the formation of the jet's shear layer and is another example of the apparent accuracy of this microphone array configuration. The mean of the distribution was 8.4 D, while the median was 9 D. Table 2 shows what percent of the noise source locations were contained within various downstream ranges of x-locations. The majority of the sound sources were located downstream of the end of the potential core (5.5 D), which matches the work done by numerous researchers as mentioned in the introduction.<sup>4-7</sup>

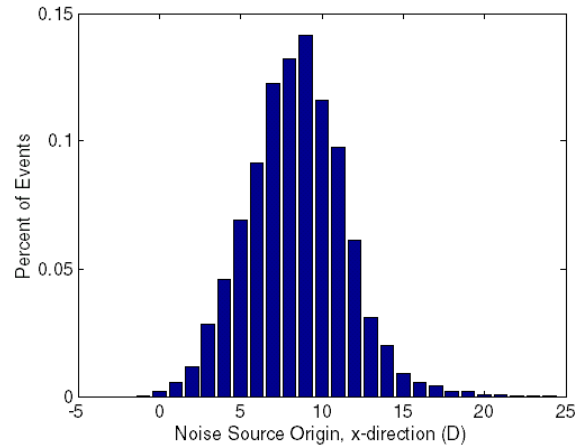


Figure 6: Probability distribution for the x-direction of the noise source locations within the Mach 1.3 jet.

Range of x-locations (D)	Percent of NSL within range
6.5 to 10.5	51
5.5 to 11.5	70
4.5 to 12.5	83
3.5 to 13.5	91
2.5 to 15.5	97
1.5 to 17.5	99

Table 2: Percent of Noise Source Locations (NSL) within different downstream ranges.

The distribution of noise source locations for various threshold levels (based on sound wave magnitude) was also computed. For a threshold of  $1.5 \sigma$ , the vast majority (70%) of noise sources was located between 5.5 and 11.5 D and almost all (99%) of the noise sources were between 1.5 and 17.5 D. If only events having a magnitude in excess of  $2.0 \sigma$  were considered (leaving 1868 noise source locations), then 75 % of the noise sources were located between 5.5 D and 11.5 D. If the minimum magnitude was increased to  $2.5 \sigma$  (702 noise source locations), then 80 % of the noise sources were located between 5.5 D and 11.5 D. Hence, the region from one to two lengths of the potential core is producing the majority of the sound at all levels between  $1.5 \sigma$  and  $2.5 \sigma$  for the Mach 1.3 jet. The length of the potential core for this jet was measured to be between 5 and 6 D.<sup>1</sup>

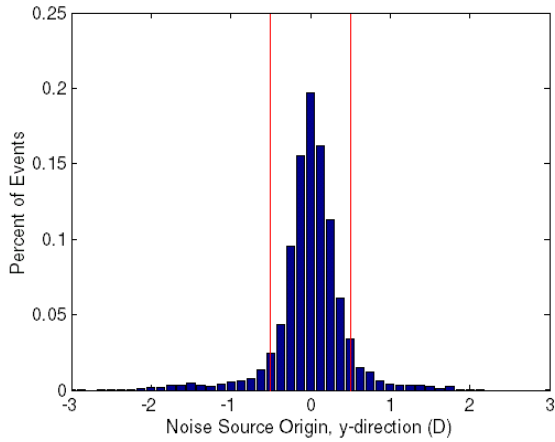


Figure 7: Probability distribution for the y-direction of the noise source locations with the Mach 1.3 jet.

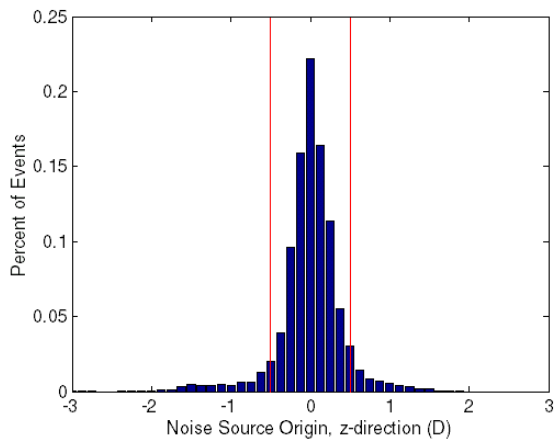


Figure 8: Probability distribution for the z-direction of the noise source locations with the Mach 1.3 jet.

The y and z component distributions of the noise source locations for the jet are shown in Figures 7 and 8. These distributions are also for a threshold

magnitude of  $1.5 \sigma$  and the bins are  $1/8 D$  in width. The vertical lines in the figures show the location of the nozzle lip line. As expected, both of the distributions are narrow. In both, over 90% of the noise source locations were located within a range that was centered on the origin with a width of  $1.25 D$ . Also as expected, the mean of the y- and z-distribution are at the jet center. Hence, the small adjustment that was made to the microphone locations based on the HTFA validation was justified as the noise source distribution is centered on the jet exit.

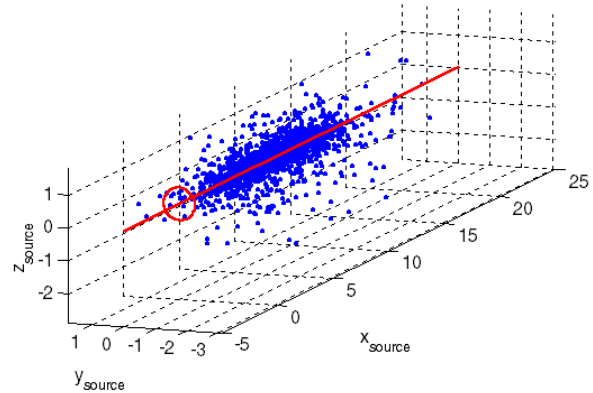


Figure 9: All noise source locations for the Mach 1.3 jet plotted in space, dimensions are in D. The circle shows the jet exit to scale while the straight line is the jet centerline.

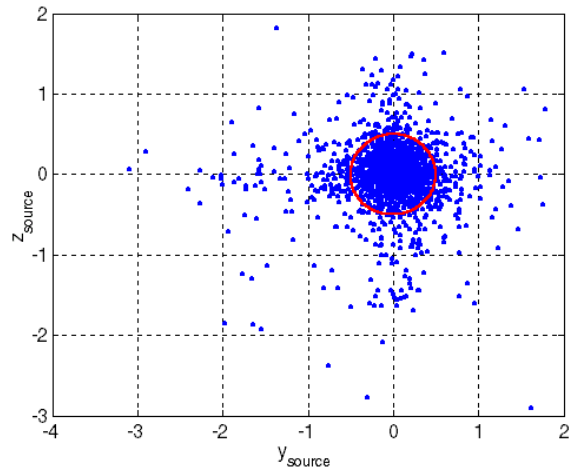


Figure 10: Figure 9 rotated so the x-axis is into the page, dimensions are in D.

In Figure 9, the noise source locations have been plotted in space. The circle at a downstream location of zero ( $x$ -source equal to zero) is the same size and location as the jet nozzle. The straight line is the jet centerline. Figure 10 shows the same data as Figure 9, but the orientation of the figure has been rotated so the x-axis is coming out of the page. As

previously mentioned in the discussion of the y and z distributions, and further shown in Figure 9 and 10, the majority of the noise source locations were within a small radial range of +/- 0.62 D.

To determine if there were any asymmetries in the nozzle with respect to the array, half of the data set was taken with the jet rotated 180°. The y and z-means for the 0° rotation were, respectively, - 0.04 and 0.01 D. The mean values for y and z with the nozzle rotated 180° were 0.05 and -0.02 D, respectively. Based on these values, there is negligible asymmetry. In summary, the 3-D array and the accompanying noise source location algorithm appear to be quite robust and accurate as they accurately predicted the location of noise sources from a HTFA and correctly placed the radial distribution of noise sources from a high-speed jet.

### Summary

Based on uncertainties in using a linear array to determine noise source origins within a high speed jet, a 3-D array was developed. The development consisted of the array hardware as well as the associated algorithm to obtain noise origins from raw microphone data. The array has an azimuthal distribution of microphones at 60° increments. At the top and bottom of the azimuthal distribution, there is an additional microphone placed 7.5 inches downstream to create inline arrays at the top and bottom of the array. The purpose of having such an arrangement is to allow the computation of all three spatial components of a noise source location using microphones that are located on the same side of the jet as the origin of the sound wave. This should reduce the impact of refraction on the predicted noise source location.

Based on a preliminary error analysis, the uncertainties in the 3-D array setup would be at most +/- 1.0 D in the streamwise component of the noise source location (x-comp. of Fig. 2). The other two components (y and z-comp. of Fig. 2) would experience negligible error. An HTFA was used to determine the accuracy of the 3-D array / noise source location algorithm. After a slight correction to the microphone locations (based on preliminary results), the location of the HTFA was predicted accurately.

The 3-D array was then used to analyze 2.5 seconds of from a Mach 1.3 jet. The origin for every sound wave that had a magnitude larger than  $1.5 \sigma$  was computed. In the streamwise direction, the vast majority (70%) of the noise sources was located between 5.5 and 11.5 D and almost all (99%) of the noise sources were between 1.5 and 17.5 D. Thus, 70 % of the noise origins were between one and two times the length of the potential core. The mean of both the

y- and z-directions was at the jet centerline, which is expected for this axisymmetric jet. Based on these results, as well as the HTFA data, the 3-D array and the accompanying noise source algorithm appear to be quite accurate in predicting noise source origins.

### Acknowledgment

This work is sponsored by the Air Force Office of Scientific Research with Drs. Steve Walker and John Schmisser as the Technical Monitors. Many fruitful discussions on the design of the array with Dr. Satish Narayanan of UTRC are greatly appreciated. The authors would also like to acknowledge Jeff Kastner for the use of the HTFA and his aid in its operation, as well as Jeff and Edgar Caraballo for their help in the development of the noise source location codes and the carrying out of the experiments. The first author would like to thank the Ohio Space Grant Consortium for his Doctoral Fellowship, and the second author would like to thank the Department of Defense for his National Defense Science and Engineering Graduate fellowship.

### References

1. Hileman, J. and Samimy, M., "Turbulence Structures and the Acoustic Far-Field of a Mach 1.3 Jet," *AIAA Journal*, Vol. 39, No. 9, 2001, pp. 1716-1727.
2. Hileman, J., Thurow, B., and Samimy, M., "An Experimental Effort on the Connection of Turbulence Structures to Far-Field Acoustic Radiation in a Mach 1.3 Jet," AIAA Paper 2001-2142, May 2001.
3. Hileman, J., Thurow, B., and Samimy, M., "Determination of Noise Sources within a high-speed Jet via Simultaneous Acoustic Measurements and real-time Flow Visualization," AIAA Paper 2001-0374.
4. Tam, C.K.W., "Jet Noise Generated by Large-Scale Coherent Motion." *Aeroacoustics of Flight Vehicles: Theory and Practice*. Vol. 1, edited by H.H. Hubbard, 1991, pp. 311-390.
5. Morrison, G.L, and McLaughlin, D.K., "Noise Generation by Instabilities in Low Reynolds Number Supersonic Jets," *Journal Sound and Vibration*, Vol. 65, 1979, pp. 177-191.
6. Yu, J.C., and Dosanjh, D.S., "Noise Field of a Supersonic Mach 1.5 Cold Model Jet," *Journal of the Acoustical Society of America*, Vol. 51, No. 5, Pt. 1, 1972, pp. 1400-1410.
7. Schaffar, M., "Direct Measurements of the Correlation Between Axial in-jet Velocity Fluctuations and Far-field Noise near the Axis of a Cold Jet," *Journal Sound and Vibration*, Vol. 64, No. 1, 1979, pp. 73-83.

8. Simonich, J., Narayanan, S., Barber, T.J., and Nishimura, M., "High Subsonic Jet Experiments Part II: Aeroacoustic Characterization, Noise Reduction & Dimensional Scaling Effects", AIAA Paper 2000-2023, 6<sup>th</sup> AIAA/CEAS Aeroacoustics Conference & Exhibit, Lahaina, Hawaii, June 2000.
9. Ahuja, K.K., Massey, K.C., and D'Agostino, M.S., "A Simple Technique of Locating Noise Sources of a Jet Under Simulated Forward Motion," AIAA Paper 98-2359, 4<sup>th</sup> AIAA/CEAS Aeroacoustics Conference, Toulouse, France, June 1998.
10. Fisher, M.J., Harper-Bourne, M., and Glegg, S.A.L., "Jet Engine Source Location: The Polar Correlation Technique," *Journal Sound and Vibration*, Vol. 51, No. 1, 1977, pp. 23-54.
11. Freund, J.B. and Fleischman, T.G., "A Numerical Study of Jet Noise Mechanisms: Sound Scattering by Turbulence," AIAA Paper 2001-0375, January, 2001.
12. Kerechanin C.W., Samimy, M., and Kim, J.-H., "Effects of Nozzle Trailing Edges on Acoustic Field of Supersonic Rectangular Jet," *AIAA Journal*, Vol. 39, No. 6, 2001, pp. 1065-1070.
13. Kastner, J. and Samimy, M., "Development and Characterization of Hartmann Tube Based Fluidic Actuators for High Speed Flow Control," AIAA Paper 2002-0128, January 2002.
14. Hartmann, J., and Trolle, B., "A New Acoustic Generator. The Air-Jet Generator," *Journal of Scientific Instruments*, Vol. 4, pp. 101-111.
15. Raman, G., Kibens, V., Cain, A., and Lepicovsky, J., "Advanced Actuator Concepts for Active Aeroacoustic Control," AIAA Paper 2000-1930.

### Appendix A: Error Analysis for the 3-D Array

We will start by assuming that the ring structure is perfectly centered on the jet centerline and the face of the ring is orthogonal to the jet centerline. The ring was designed with an inner radius of 30.000 +0.000 / -0.010 inches, and the individual microphones were all at a fixed distance from this inner surface. The microphone locations from the ring inner surface were all 4.000 +/- 0.010 inches (a set of 6 inch calipers was used for these measurements). The distance between the grid cover top (where these measurements were made) and the diaphragm face were also measured. These values were then added to the radial locations of the microphones. Therefore, the radial distance from each of the microphone diaphragms to the center of the ring was 26.050 +0.015 / -0.015 inches.

The distance from the front of the ring to the center of the microphones could also be precisely measured. The four azimuthally mounted microphones (microphones 3, 4, 5, and 8 in Figure 2) were held into the ring by extension posts. These posts were in set holes with a depth held to 0.100 +/- 0.005 inches, this same dimension was used on the set holes within the mounts. All of the extension posts had the same height of 1.400 +/- 0.002 inches, and the distance between the microphone centerline and the mount set hole was held to 0.650 +/- 0.004 inches. Therefore, the space between the face of the ring and the centers for these four microphones was 1.850 +/- 0.02 inches. Since the inline microphones are not directly mounted to the ring (they are connected to the ring mounts), their positions needed to be measured, and they were 1.942 and 1.987 inches, respectively for the top and bottom. These measurements are accurate to within 0.02 inches. The locations for the top and bottom front microphones (numbers 1 and 6 in Figure 2) were offset from the other azimuthally mounted microphones by -0.092 and -0.137 inches, respectively in the noise source location codes. The centers for the four azimuthally mounted microphones were used as the reference point for the measurement of the downstream distance from the jet exit to the array. The random downstream error in the measurement of any of front six microphones was set as +/- 0.02 inches. The inline microphones were held in an aluminum block where the distances between mounting holes was held to +/- 0.002 inches. Hence, the rear inline microphones were located 7.500 +/- 0.002 inches behind the front inline microphones.

The azimuthal spacing in the machining of the ring was held to a tolerance of 20 seconds of a degree for every 10° of hole spacing. Therefore, the microphones that were spaced 60° apart had an

uncertainty of 120 seconds, which is negligible (60° is the maximum azimuthal spacing used in the nsl routine). The space between the sets of mounting holes and the extension posts had minimal clearance, and as there were two holes, this should not add at most a tenth of a degree of uncertainty. The azimuthal spacing was set as 60° +/- 0.1°.

The combined effect for these errors was determined by using a set of time separations that without any errors gave a noise source location of [8.52 0.02 0.00] and then varying the errors until a maximum offset from the original noise source location was achieved. The errors will be configured to get a noise source location that is as far upstream from the zero-error source as possible. This configuration of errors consisted of errors in each microphone's location. The radial direction varied by 0.015 inch, the downstream by 0.020 inch, the azimuthal spacing by 0.1° and the inline separation by 0.002 inch. For this set of error sources, the worst-case scenario noise source location was [8.11 0.01 0.00]. This deviates from the original case by a minimal amount in the y and z directions and by 0.4 inches in the x direction.

The anechoic chamber temperature was measured using an Omega handheld thermometer. The quoted uncertainty for the device is +/- 2°F. A positive 2°F would change the speed of sound within the chamber and cause a change in the predicted noise source location to [7.85 0.01 0.00].

The data was acquired at a rate of 1 MHz. Hence, there is +/- 1 µsec uncertainty in any of the time delay measurements. These uncertainties can be combined with those given previously to yield a noise source location of [7.58 0.03 0.02]. Thus, if all of the random variations in the measurements were combined into a worst-case scenario, the noise source location would be offset by 0.94 D in the x-direction and by a few hundredths of an inch in the y and z-directions. Apparently, these uncertainties have a much larger affect in the x-direction calculations than in the y or z.

The errors from the second listed item are less quantifiable than the first set. This is because they are measurements made relative to the jet centerline, which in our facility, is not easily measured to the accuracy of the first set of errors. The relative position of the ring with respect to the jet centerline was determined using two strings that were sent through microphone holes within opposite azimuthal mounts. The distance from where the strings crossed and the center of the jet nozzle could then be measured giving the downstream

location of the microphones. These strings were then centered on an additional string that passed closely through the jet centerline. This should center the ring in the y and z directions. The uncertainty in the x-direction placement was estimated as 1/8 inch, which can be added to the uncertainty from the previous paragraph to give a worst case uncertainty of 1.0 D.

The offset in the y and z directions was unknown. Fortunately, the y and z offsets (deviation from the ring and jet centers) were later determined by performing a validation with a Hartmann tube fluidic actuator and confirmed by applying knowledge that a round jet should have an average symmetric distribution of noise sources.

## Appendix B: HTFA Validation

The HTFA used for the validation of the ring array is based on the design described in Kastner and Samimy (2002). The converging nozzle of the HTFA had an exit diameter of 6 mm and the shield provided a set distance between the nozzle exit and the entrance of the tube of 8 mm. In the work of Kastner and Samimy (2002), tube depths of 6, 12, and 18 mm (1, 2, and 3 nozzle diameters) were tested via near field pressure, far-field acoustic, and flow visualization measurements. The frequency of the far-field tone created by the HTFA decreases with increasing tube length. For a tube length of 18 mm, the frequency of the fundamental was measured as 3.4 kHz.<sup>13</sup> A lower frequency was desired for the validation, so a tube with a length of 36 mm (6 nozzle diameters) was built for the HTFA.

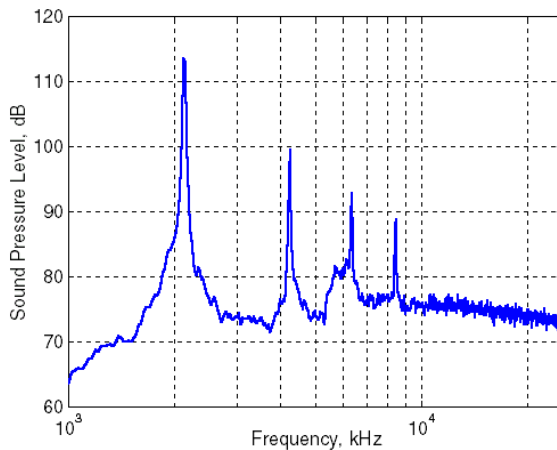


Figure 11: Hartmann tube far field sound spectrum. Measurement made with microphone 1 when tube was aligned with z-axis.

The far-field sound pressure level for the HTFA is presented in Figure 11. The HTFA was operated at a line pressure of 54 psi with the 36 mm tube. The sound data was taken at a sampling frequency of 100 kHz with low pass filtering at 30 kHz. The spectrum is the ensemble average of 100 blocks of 4096 samples. The fundamental frequency was 2124 Hz and there were three harmonics present. This pure tone is quite different from the broadband noise that is created by the Mach 1.3 jet. The average waveforms for the HTFA and the Mach 1.3 jet also differ considerably (compare Kastner and Samimy, 2001 to Hileman et al., 2001). However, the authors have not found a noise source that is as small as the HTFA that can produce the same frequency content as the Mach 1.3 jet. Therefore, the pure tone generating HTFA was used for the validation.

The HTFA was placed downstream of the Mach 1.3 jet nozzle exit with the 3-D array configured as it would be when it would be taking jet noise data. The open part of the HTFA was pointing in the positive x-direction (see Figure 7 for orientation) while the tube was aligned with the z-direction. The opening of the HTFA was 5.4 D downstream of the origin, which is at the nozzle exit plane, with the center of the opening of the HTFA located on the jet nozzle centerline. For noise source location calculations, 20 blocks of 16384 data points were taken at a sampling rate of 1 MHz. Low pass filtering was set at 100 kHz.

The noise source locations were processed for all sound waves that had a magnitude in excess of  $1.5 \sigma$  (standard deviation of the sound pressure). This gave about 900 individual noise source. The probability distribution for the x-direction case has been plotted in Figure 12. It shows that almost all of the noise sources were located between 5.5 and 6.75 inches downstream of the jet nozzle exit. This is expected since the opening of the HTFA was located at 5.4D. The flow visualization images of Kastner and Samimy (2002) of a similar HTFA showed significant vortical flow activity over the entire opening of the HTFA and extending significantly away from the opening.

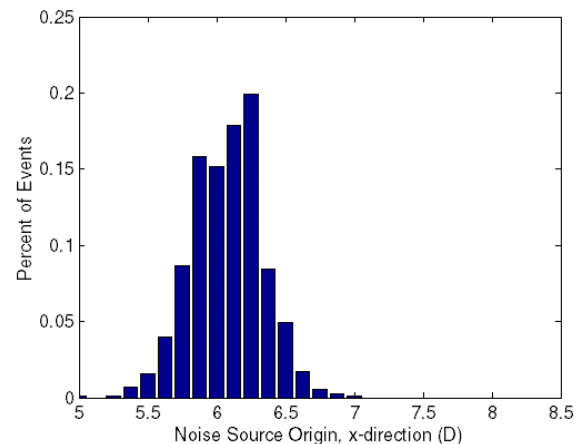


Figure 12: Probability density distribution of the noise source location in the x direction with the HTFA aligned with the z-axis.

The y and z-direction probability distributions for the HTFA are shown in Figures 13 and 14. The vertical lines in the figures show the location and size of the opening of the HTFA. In Figure 13, the distribution is quite narrow. Each bin is  $1/16 D$  wide, thus the distribution is only  $0.38 D$  wide, which is slightly larger than the 8 mm opening of the HTFA. However, the center of the distribution has a slight

positive offset from the center of the HTFA opening. Figure 14 shows a similar distribution for the z-direction. Again, the distribution is about 0.38 D wide, and it is offset in the positive direction.

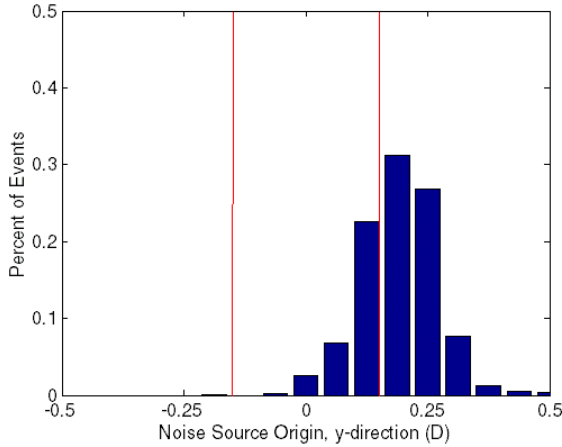


Figure 13: Probability density distribution of the noise source location in the y direction with the HTFA aligned the with z-axis.

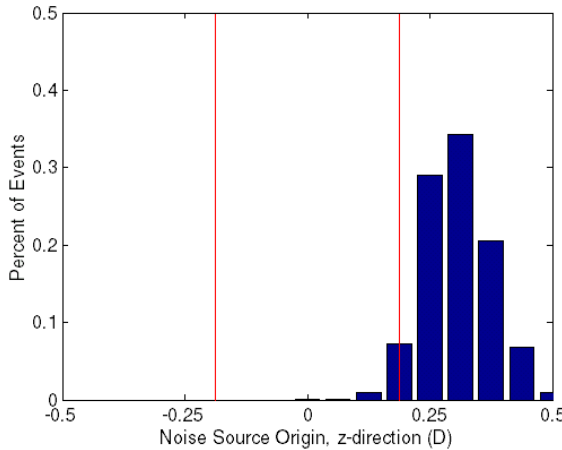


Figure 14: Probability density distribution of the noise source location in the z direction with the HTFA aligned with the z-axis.

Every noise source location for the z-coordinate aligned case has been plotted in three-dimensional space in Figure 15. The axes of the figure are the same as those used in the probability density distributions of Figures 12-14. The box in the central portion of the Figure marks the opening of the HTFA. The arrow within the converging nozzle shows the direction the air is blowing. The resonance tube is on the opposite side of the box from the converging nozzle and arrow. Figure 16 shows Figure 15 rotated so the x-coordinate goes into the page. As was observed in Figures 13 and 14, all of the noise sources are located slightly above and to the left of the opening with Figure 16.

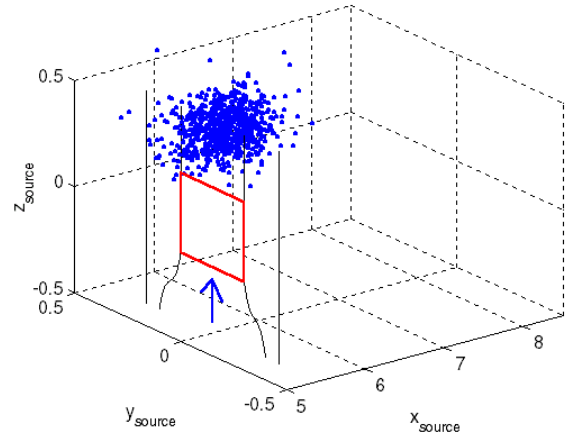


Figure 15: All noise source locations for the HTFA plotted in space, dimensions are in D. The central box shows the opening of the HTFA.

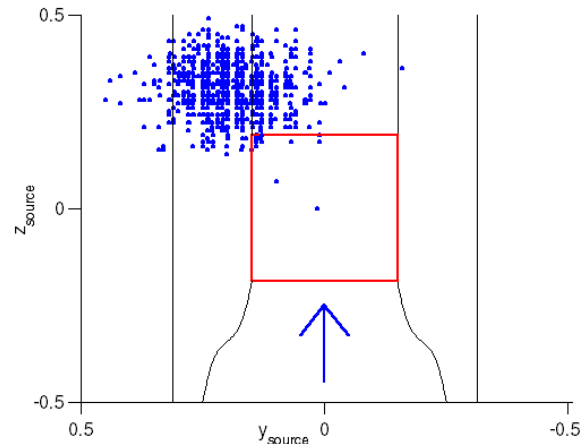


Figure 16: Figure 15 rotated so the x-axis is into the page, dimensions are in D.

The small discrepancy in the y and z distributions likely originates within the array setup or in the data processing. The most likely explanation for the small offset in the y and z distributions is the center of the 3-D array was offset from the jet centerline by these small distances. The 3-D array projects noise sources onto a set of orthogonal coordinates where the x-coordinate passes through the center of, and is perpendicular to, the plane that is formed by the azimuthal distribution of microphones. Hence, if the center of the ring were offset from the center of the nozzle, then there would be an equal offset in the location of each noise source location.

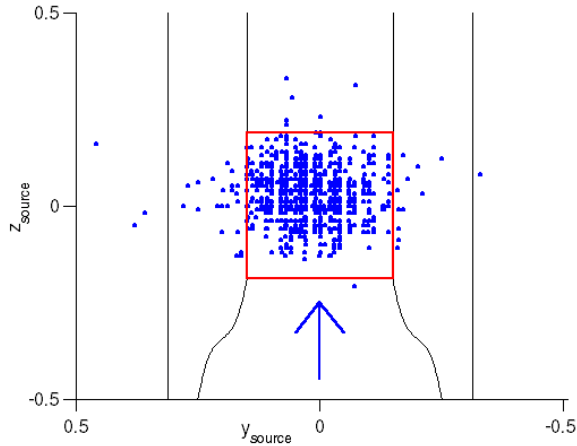


Figure 17: All noise source locations for the HTFA plotted in space, dimensions are in  $D$ . The microphone locations were shifted as discussed in the text.

The location for each of the microphones was modified by the small offsets in the mean of the  $y$  and  $z$  distributions from the HTFA. The  $y$ -location of each microphone was shifted  $-0.17 D$  while the  $z$ -location was shifted  $-0.28 D$  and the noise source location were recomputed. With this correction, the means of both the  $y$  and  $z$ -distributions was  $0.02$ . Figure 17 is a plot similar to Figure 16, but the noise source locations are those that were recomputed with the corrected microphone positions. The small corrections cause the noise sources to move to the expected location over the opening of the HTFA. Further, the means of the  $y$  and  $z$ -distributions were reduced to  $0.02 D$  and  $0.03 D$ , respectively. These corrections to the  $y$  and  $z$  locations of the microphones within the ring array were also applied to the data from the Mach 1.3 jet